

Research Article

<https://doi.org/10.1631/jzus.A2200599>



Short-term tunnel-settlement prediction based on Bayesian wavelet: a probability analysis method

Yang DING^{1,2,3}, Xiaowei YE⁴, Zhi DING¹, Gang WEI¹, Yunliang CUI¹, Zhen HAN⁵, Tao JIN^{3✉}

¹Key Laboratory of Safe Construction and Intelligent Maintenance for Urban Shield Tunnels of Zhejiang Province, Hangzhou City University, Hangzhou 310015, China

²Zhejiang Engineering Research Center of Intelligent Urban Infrastructure, Hangzhou City University, Hangzhou 310015, China

³Department of Civil Engineering, Hangzhou City University, Hangzhou 310015, China

⁴Department of Civil Engineering, Zhejiang University, Hangzhou 310058, China

⁵Nanjing Metro Operation Co., Ltd., Nanjing 210012, China

Abstract: As urbanization accelerates, the metro has become an important means of transportation. Considering the safety problems caused by metro construction, ground settlement needs to be monitored and predicted regularly, especially when a new metro line crosses an existing one. In this paper, we propose a settlement-probability prediction model with a Bayesian emulator (BE) based on the Gaussian prior (GP), that is, a GPBE. In addition, considering the distortion characteristics of monitoring data, the data is denoised using wavelet decomposition (WD), so the final prediction model is WD-GPBE. In particular, the effects of different prediction ratios and moving windows on prediction performance are explored, and the optimal number of moving windows is determined. In addition, the predicted value for GPBE based on the original data is compared with the predicted value for WD-GPBE based on the denoised data. One year of settlement-monitoring data collected by a structural health monitoring (SHM) system installed on the Nanjing Metro is used to demonstrate the effectiveness of WD-GPBE and GPBE for predicting settlement.

Key words: Metro construction; Settlement probability prediction; Structural health monitoring (SHM); Wavelet denoising; Gaussian prior (GP); Bayesian emulator (BE)

1 Introduction

Metro is an important part of urban rail transit (Cheng et al., 2020; Qu et al., 2023). In recent years, it has become the trend in urban development, and is an effective way to solve urban traffic congestion, save energy, and reduce pollution. However, the ground settlement caused by its construction process is an urgent problem to be solved (Kong et al., 2020; Liang et al., 2022). For example, on Mar. 28, 2007, construction of Beijing Metro Line 10 resulted in the collapse of the project. On July 1, 2003, construction of Shanghai Metro Line 4 caused a high-rise building to collapse. The sand layer of Qingdao Metro Line 2 collapsed on

Apr. 13, 2018 (Wu et al., 2018). Sysyn et al. (2021b) studied the mechanism of sleeper-ballast dynamic impact in the void zone. The results of experimental in situ measurements of rail deflections showed significant impact accelerations in the zone even for light-weight, slow vehicles. Furthermore, the group presented theoretical and experimental studies directed at the development of methods for sleeper-support identification (Sysyn et al., 2020a). Among other approaches, they used track-side and on-board monitoring methods to avoid or delay the development of local instabilities such as ballast breakdown, white spots, and sub-grade defects. For example, they used high-speed video-recording and digital-imaging correlation methods to measure dynamic rail displacements (Sysyn et al., 2021a). In addition, they proposed a practical method of void parameter quantification (Sysyn et al., 2020b). Obviously, irregular rates of settlement will lead to an increase in maintenance costs, thereby affecting the

✉ Tao JIN, jintao@hzcu.edu.cn

 Yang DING, <https://orcid.org/0000-0002-1298-1710>

Received Dec. 20, 2022; Revision accepted May 27, 2023;
Crosschecked Oct. 23, 2023

© Zhejiang University Press 2023

reliability and availability of transportation. Therefore, it is necessary to conduct long-term monitoring of settlement and predict it based on massive data to avoid potential accidents.

At present, structural health monitoring (SHM) systems are mainly used for real-time monitoring of settlement; these include level gauges, strain gauges, and other sensors that can obtain real data (Ng et al., 2013; Gómez et al., 2020). For settlement prediction, theoretical analysis methods and machine learning methods are used (Samui, 2008; Yao et al., 2018; Li et al., 2021). For example, Mu et al. (2021) used the numerical model to simulate and predict the tunneling deformation of Foshan Metro Line 2, and compared it with the monitoring data. Qu et al. (2021) combined the measured deformation data with the circular sliding theory to study the deformation based on the limit equilibrium method. Xiang et al. (2008) estimated the possible additional settlement of pile foundation using empirical and theoretical analysis and numerical simulation of the construction process.

Obviously, the expressions of theoretical prediction models are complex and difficult to solve. In addition, a large number of soil parameters are required, which increases the uncertainty of the predicted value (Liu et al., 2022; Wang et al., 2022; Ding et al., 2023e, 2023f). In contrast, the settlement-prediction model based on machine learning algorithms only requires settlement data, that is, the machine-learning algorithm can fully mine the information from the data and then predict the next settlement value (Gong et al., 2014; Li et al., 2019; Ye et al., 2019, 2020; Ding et al., 2023c). Machine-learning prediction models are primarily divided into two categories: deterministic prediction and uncertain prediction (Chitsazan et al., 2015; Chen et al., 2019; Law et al., 2020). For deterministic methods, the predicted settlement is a definite value, while for the uncertain method, it is an interval value. For example, Ji et al. (2014) proposed a time-series method based on least square support vector regression (LSSVR) to predict dynamic lateral deformation and surface subsidence of support structures in deep foundation pit engineering. Wang et al. (2013) used the smooth correlation vector machine with wavelet kernel to study how the land subsidence caused by tunnel excavation develops. Shahin et al. (2005) presented the uncertainties associated with settlement prediction and combined Monte Carlo simulations with deterministic

neural network models to obtain possible distributions of predicted settlements.

The SHM system faces two major difficulties during operation, namely that it powers off, which leads to data loss, and it is subjected to external interference, which leads to data distortion (Farrar et al., 2006). Therefore, it is necessary to reduce noise and supplement monitoring subsidence data. Tay (2021) developed a recursive graph median filter that can be highly localized and implemented through distributed processing. Huang et al. (2019) proposed a new approach that combines displacement entropy and spectral substitution with integrated empirical mode decomposition (EMD). Jiang et al. (2007) developed a Bayesian discrete wavelet packet transform denoising method and studied the influence of noise in measured data on structural system identification. Zhang et al. (2017) proposed a new hybrid approach that integrates wavelet packet transform and an LSSVM to improve the accuracy and reliability of daily tuning-induced land-settlement estimates. Ding et al. (2011) established a stochastic model and regarded the settlement data as a time series and the measurement error as a stable and normally distributed random process.

In this study, a settlement-probability prediction model is established with a Bayesian emulator (BE) based on the Gaussian prior (GP), that is, a GPBE. Specifically, the BE probability prediction model is derived based on the Bayesian theorem and GP. The original settlement-monitoring data are denoised based on wavelet decomposition (WD), and thus the final model is WD-GPBE. The application of GPBE and WD-GPBE models of settlement is verified based on SHM data collected from the Nanjing Metro.

2 Methodology

2.1 Wavelet decomposition method

In general, monitoring sequence data has waveform characteristics, while real-time sequence data has repeatability characteristics (Sandham et al., 1998). Therefore, sequence data can be represented as an infinite waveform function (He et al., 2010). The WD method decomposes monitoring data step by step by way of high and low frequencies, that is, it decomposes time-series data by wavelet function (Wang and van der Schaar, 2006):

$$\begin{aligned} \psi(t) &= \frac{1}{\sqrt{a}} \psi\left(\frac{t-b}{a}\right), \\ a &= 2^j, \\ b &= k \times 2^j, \end{aligned} \tag{1}$$

where t is the time, a is the scale factor, b is the translation factor, j is the scale coefficient, and k is the translation coefficient.

By setting the threshold T for the above wavelet coefficients, the high-frequency data in the monitoring data can be filtered out; the noise information contained in the wavelet function which surpasses the threshold is completely eliminated (Hashemi and Beheshti, 2014). Nowadays, the Bayes Shrink threshold-estimation method is used to determine the threshold (Sendur and Selesnick, 2002). With this method, the wavelet function is modeled based on the statistical characteristics, and then the threshold T is obtained according to Bayesian estimation (Hashemi and Beheshti, 2010):

$$T = \frac{\sigma_n^2}{\sigma_w}, \tag{2}$$

where σ_n is the standard deviation of noise, and σ_w is the standard deviation of the initial wavelet function.

2.2 Bayesian emulator

The BE is a probability model based on Bayesian theory, which can be expressed by

$$\begin{aligned} p(A|B) &= \frac{p(A, B)}{p(B)} = \\ &= \frac{p(A) p(B|A)}{p(B)} \propto p(A) p(B|A), \end{aligned} \tag{3}$$

where $p(A|B)$ is the a posteriori probability of event A, $p(A, B)$ is the probability of both event A and event B occurring simultaneously, $p(B|A)$ is the likelihood function, $p(A)$ is the a priori probability of event A, and $p(B)$ is a constant (Ni et al., 2020; Ding et al., 2023g).

Furthermore, when there are n random events, that is, A_1, A_2, \dots, A_n , then

$$p(A_i|B) = \frac{p(A_i, B)}{p(B)} = \frac{p(A_i) p(B|A_i)}{\sum_{i=1}^n p(A_i) p(B|A_i)}. \tag{4}$$

2.3 Gaussian prior

As can be seen from Bayesian theory, we need the a priori probability and the likelihood function of events. The a priori probability can be expressed by Gaussian distribution, that is, the GP (Ding et al., 2023a). When the value of observation output \mathbf{Y} is given, the posterior distribution of prediction output f_* can be expressed as follows (Ding et al., 2023c, 2023f):

$$p(f_*|\mathbf{Y}) = \int p(f, f_*|\mathbf{Y}) df = \frac{1}{p(\mathbf{Y})} \int p(f, f_*) p(\mathbf{Y}|f) df. \tag{5}$$

When all parameters in Eq. (5) can be expressed by Gaussian distribution, the posterior distribution of prediction output can also be expressed by Gaussian distribution, that is, by a GPBE prediction model (Ye et al., 2021; Ding et al., 2023b).

$$\begin{aligned} p(f_*|\mathbf{Y}) &= \mathcal{N}(\mu_{f_*}, \sigma_{f_*}^2), \\ \mu_{f_*} &= \mathbf{C}_* \mathbf{K}^{-1} \mathbf{Y}, \\ \sigma_{f_*}^2 &= \tilde{\mathbf{C}} - \mathbf{C}_*^T \mathbf{K}^{-1} \mathbf{C}_*, \end{aligned} \tag{6}$$

where \mathbf{C} is the covariance function, $\mathbf{K} = \mathbf{C} + \sigma_n^2 \mathbf{I}_n$, $\mathbf{C} = \mathbf{C}(\mathbf{X}, \mathbf{X})$, $\mathbf{C}_* = \mathbf{C}(x_*, \mathbf{X})$, $\mathbf{X} = \{x_i\}_{i=1}^n$, $\mathbf{Y} = \{y_i\}_{i=1}^n$, $\mathbf{f} = \mathbf{f}(\mathbf{X})$, $f_* = f(x_*)$, $\tilde{\mathbf{C}} = \mathbf{C}(x_*, x_*)$, $p(\mathbf{f}, f_*) = \mathcal{N}\left(\begin{bmatrix} \mathbf{0} \\ \mathbf{0} \end{bmatrix}, \begin{bmatrix} \mathbf{C} & \mathbf{C}_* \\ \mathbf{C}_*^T & \tilde{\mathbf{C}} \end{bmatrix}\right)$, and \mathbf{I}_n is an identity matrix of $n \times n$.

In addition, it can be seen from Eq. (6) that determination of the covariance function is the key to calculating the predicted value. Possible approaches include the squared-exponential (SE) method, Matern (MA) covariance function, and periodic (PE) covariance function. Here, we select SE covariance function to derive the mean and variance of the predicted value, that is,

$$C_{SE}(x, x') = \eta^2 \exp\left[-\frac{(x-x')^2}{2\ell^2}\right], \tag{7}$$

where η^2 is the signal variance, and ℓ is the characteristic length scale. An implication of the SE correlation function is that the resulting sample functions are infinitely differentiable, expressing an assumption that the process to be modeled is very smooth.

The SE covariance function is clearly smooth, that is, with continuous variable X input, the output curve is very smooth, without singular characteristics.

Therefore, when the original data is processed by the WD method, it can be perfectly combined with the GPBE.

3 Illustrative application: Zhongsheng Station of Nanjing Metro

Tunnel-settlement monitoring is a necessary method of understanding and controlling changes in tunnel structure, finding dysfunction in time, and judging the safety risks. During operation, due to the reciprocating movement of subway trains, dynamic fatigue load will form, leading to settlement of the tunnel. Therefore, real-time monitoring of settlement is needed. During the maintenance phase, when the settlement value returns to the safe range after reinforcement measures, maintenance can be stopped and the tunnel can continue to operate. The early warning index of subsidence is formulated according to the technical specification for safety protection of urban rail transit structure (MOHURD, 2013) and monitoring regulation of urban rail transit engineering of Jiangsu Province of China (Jiangsu Provincial Department of Housing and Urban Rural Development, 2015). Once the early warning value is exceeded, the tunnel needs to be reinforced and maintained. Therefore, sedimentation can be used as a preventive index during operation. In the maintenance phase, it can be used as a target indicator.

The Zhongsheng Station on the new Nanjing Metro Line 7, which is planned to open to traffic in 2023, crosses the existing Zhongsheng Station of Metro Line 10, with a station scale of $270\text{ m}\times 21.9\text{ m}\times 21.1\text{ m}$ (Ding et al., 2023d). The Zhongsheng Station, on the existing Metro Line 10, was completed in 2004, and the initial value monitoring during the operation period was completed in Aug. 2005. The SHM system at Zhongsheng Station includes 31 settlement-monitoring points before the construction of Metro Line 7 (J1–J31) and four settlement-monitoring points after the construction of Metro Line 7 (M1–M4) (Ding et al., 2023b). The reinforced and existing columns and monitoring system at Zhongsheng Station are shown in Fig. 1.

Therefore, the settlement of monitoring points M1–M4 can represent the impact of the new metro on the existing metro. The original settlement-monitoring data from Mar. 19, 2021 to Jan. 19, 2022 is shown in Fig. 2a (Ding et al., 2023b) and the denoised data

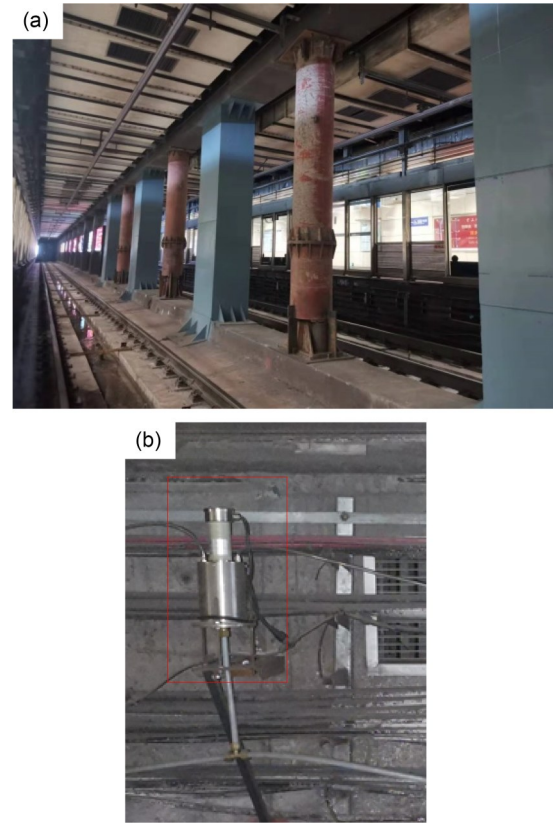


Fig. 1 Photographs at Zhongsheng Station: (a) reinforced columns (M1–M4) and existing columns (J1–J31); (b) monitoring system. The distance between adjacent existing columns is 10 m, and the distance between adjacent existing and reinforced columns is 5 m

from Mar. 19, 2021 to Jan. 19, 2022 is shown in Fig. 2b. It can be seen from Fig. 2 that the settlement value at the monitoring point first increases and then decreases, that is, the settlement value in the growth phase is about 1.0–3.0 mm, while it is about 1.0–1.5 mm in the stable stage. This is because the settlement value increases due to disturbance of excavation construction in the growth stage. In order to avoid excessive settlement, the operation unit reinforced the column by the metro jet system (MJS) method and established subway protection measures, so as to control settlement changes and stabilize the tunnel. By comparing Figs. 2a and 2b, we can see that the settlement curve was smoother after noise reduction by the WD method; the WD method was able to delete anomalous data present in the monitoring data.

In the settlement-prediction probability model based on GPBE, there are two key parameters that need to be determined: prediction ratios and the moving

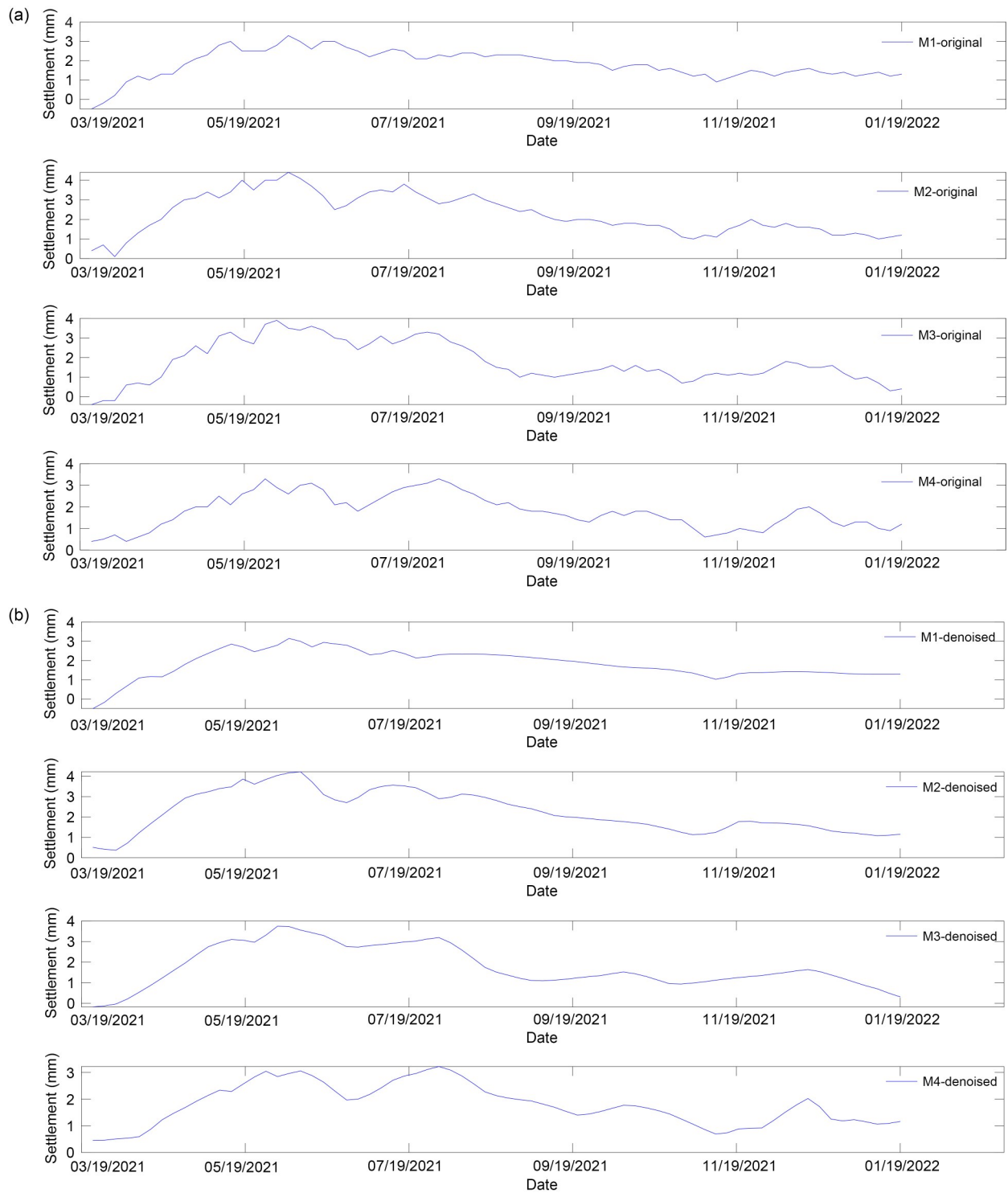


Fig. 2 Settlement data for M1–M4: (a) original data (Ding et al., 2023b); (b) denoised data

window. The prediction ratios are the proportion of the predicted ratios in the data set. The moving window is the correlation between the settlement value and the first n data; n indicates the moving window. For example, when the moving window is 10, the first 10 data values

are selected to predict the next data values. Also, the prediction curve is drawn by starting from the 11 original data points, which leads to the starting points of the x -axis in the prediction curve and original data being different.

In this section, we discuss the influence of different moving windows and prediction ratios on the prediction performance of the proposed model. When the moving window is 1 and the predicted ratio is 1%, the prediction results based on the GPBE model are as shown

in Fig. 3. Specifically, Fig. 3a shows the prediction results for the original data, and Fig. 3b shows the prediction results for the denoised data.

Similarly, when the moving window is 1 and the predicted ratio is 5%, the prediction results of the GPBE

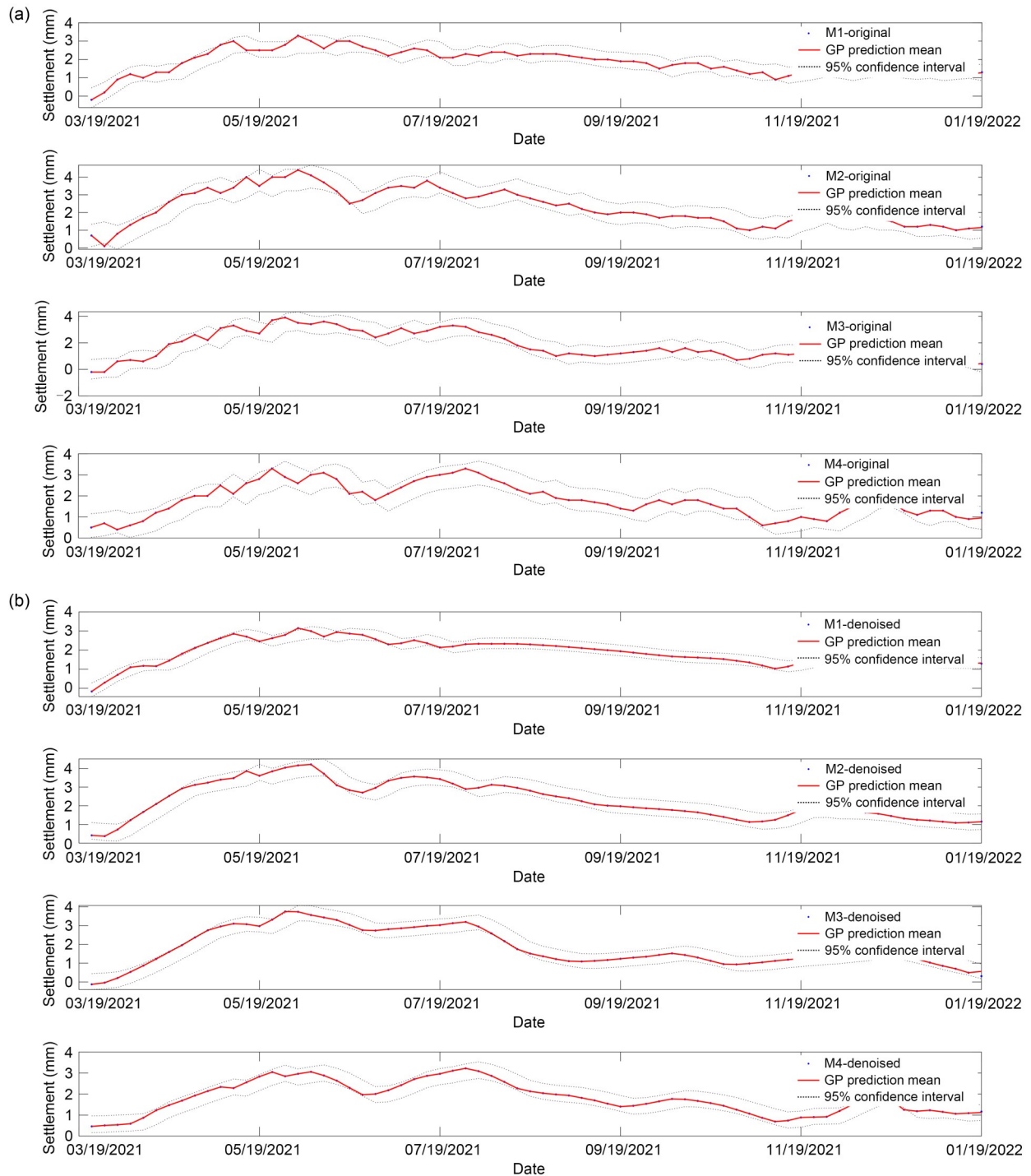


Fig. 3 Settlement probability prediction with a moving window of 1 and predicted ratio of 1%: (a) probability prediction based on original data; (b) probability prediction based on denoised data

model are as shown in Fig. 4. Fig. 5 shows the prediction results with a moving window of 1 and predicted ratio of 10%. Fig. 6 shows the prediction results with a moving window of 5 and predicted ratio of 1%. With a moving window of 5 and a predicted ratio of 5%, the prediction

results are as shown in Fig. 7. When the moving window is 5 and the predicted ratio is 10%, the prediction results based on GPBE model are shown in Fig. 8. When the moving window is 10 and the predicted ratio is 1%, the prediction results based on GPBE model are shown in

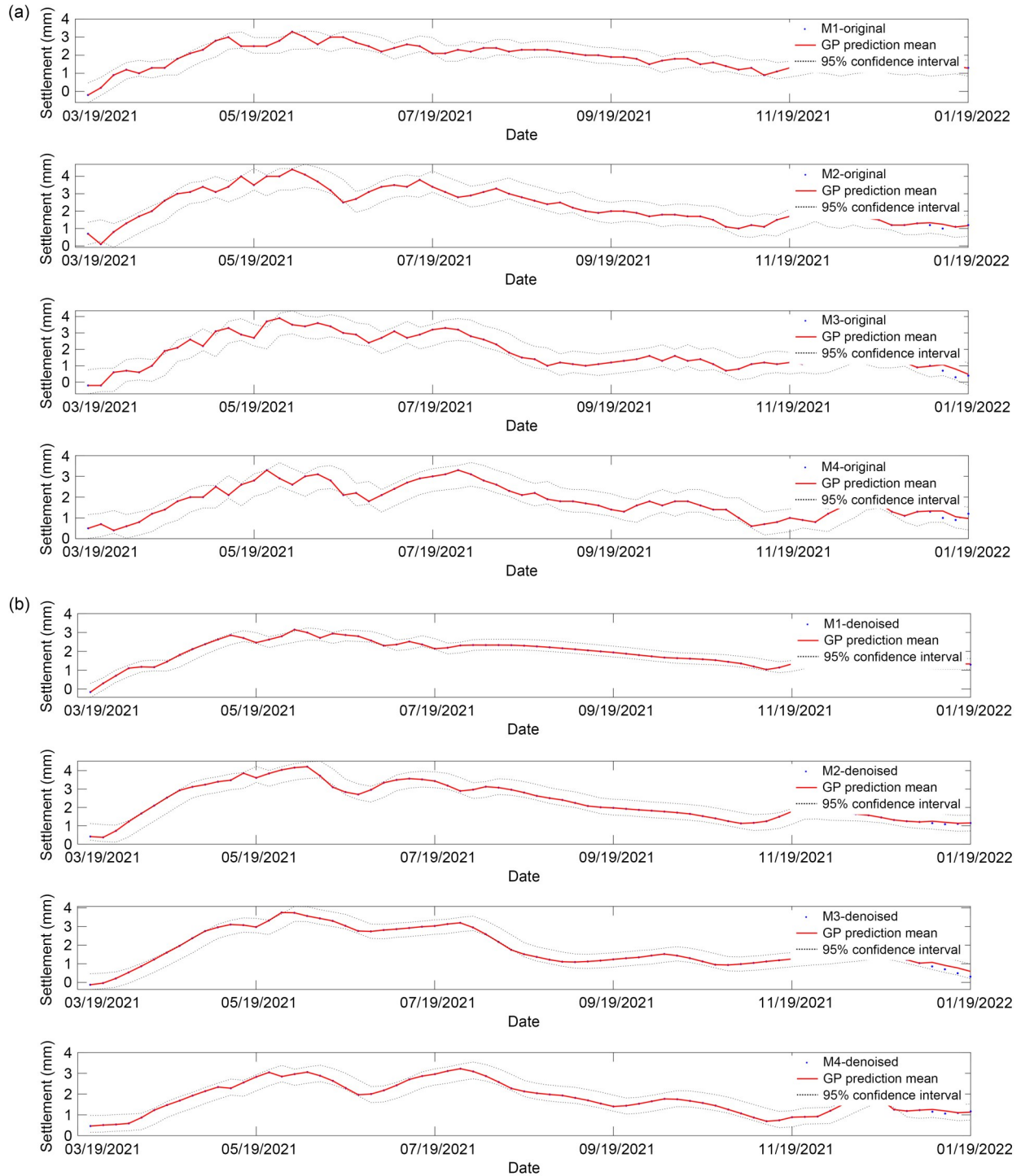


Fig. 4 Settlement probability prediction with a moving window of 1 and predicted ratio of 5%: (a) probability prediction based on original data; (b) probability prediction based on denoised data

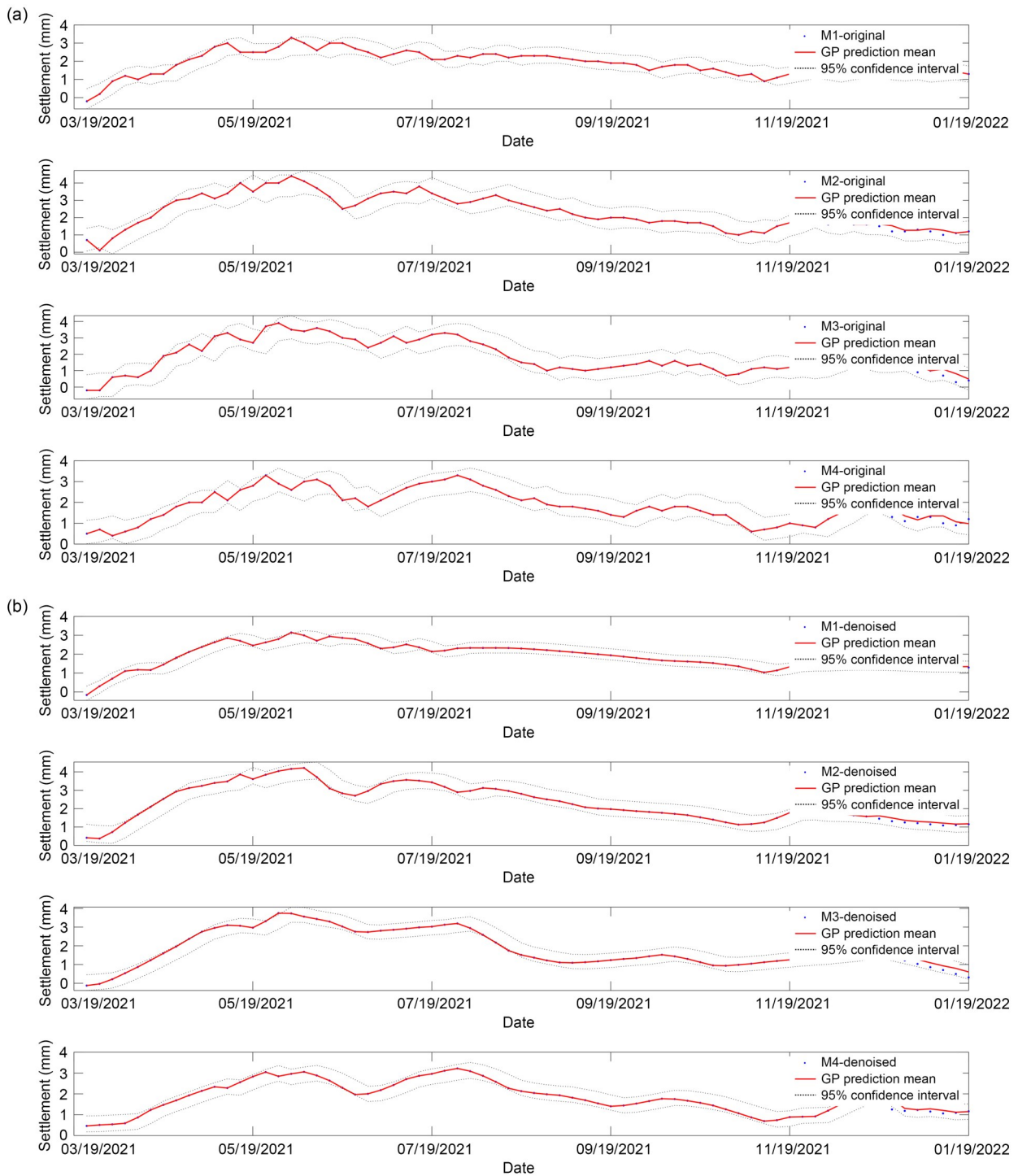


Fig. 5 Settlement probability prediction with a moving window of 1 and predicted ratio of 10%: (a) probability prediction based on original data; (b) probability prediction based on denoised data

Fig. 9. When the moving window is 10 and the predicted ratio is 5%, the prediction results based on GPBE model are shown in Fig. 10. When the moving window is 10 and the predicted ratio is 10%, the prediction results based on GPBE model are shown in Fig. 11.

It is clear from these figures that the proposed GPBE probability prediction method satisfactorily describes the variation law of settlement and gives a 95% confidence interval to the settlement value. In other words, the predicted settlement values are in the 95%

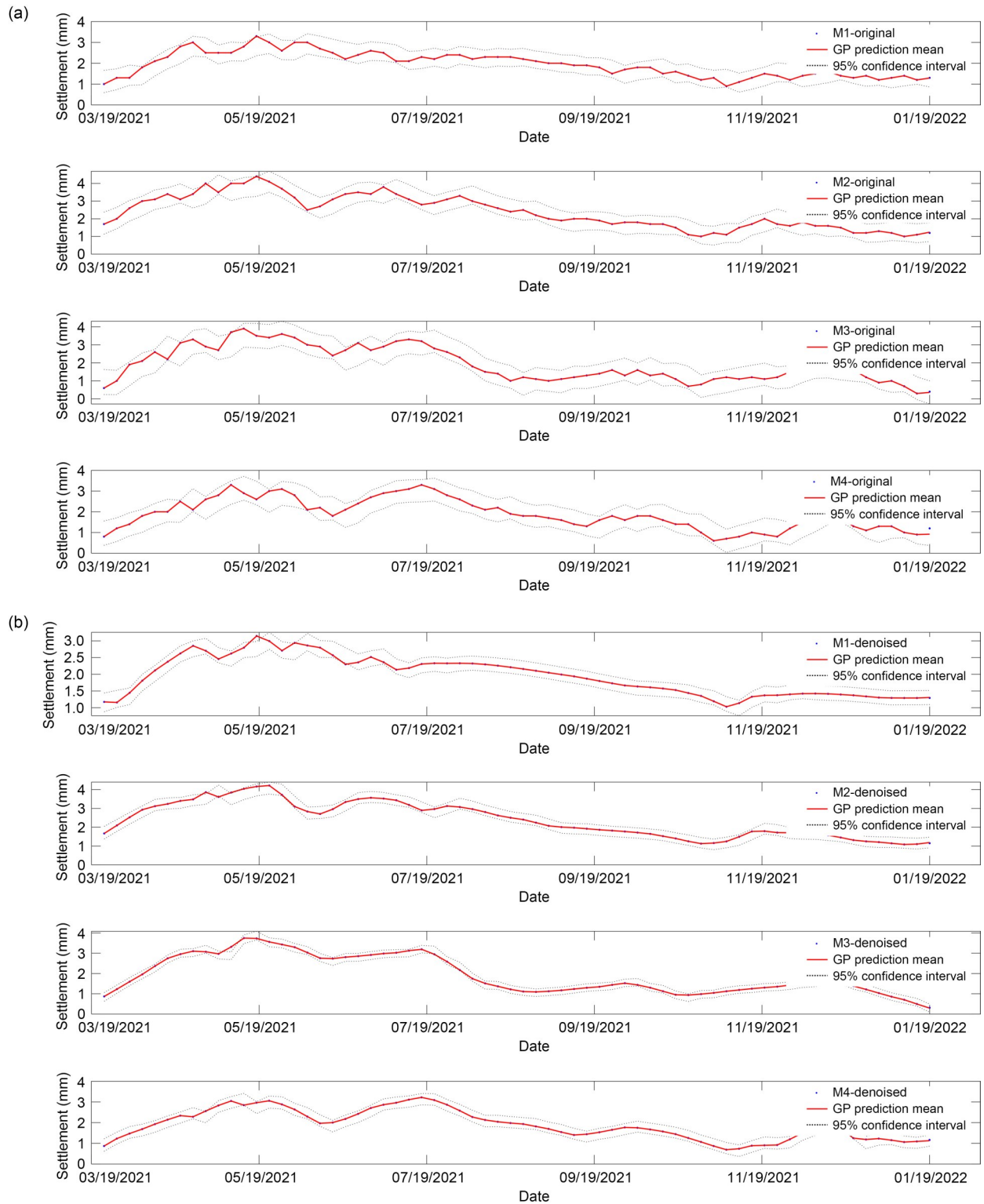


Fig. 6 Settlement probability prediction with a moving window of 5 and predicted ratio of 1%: (a) probability prediction based on original data; (b) probability prediction based on denoised data

confidence interval, which fully consider the uncertainty of settlement data.

In addition, the root mean square error (RMSE) is used to assess the performance of the prediction

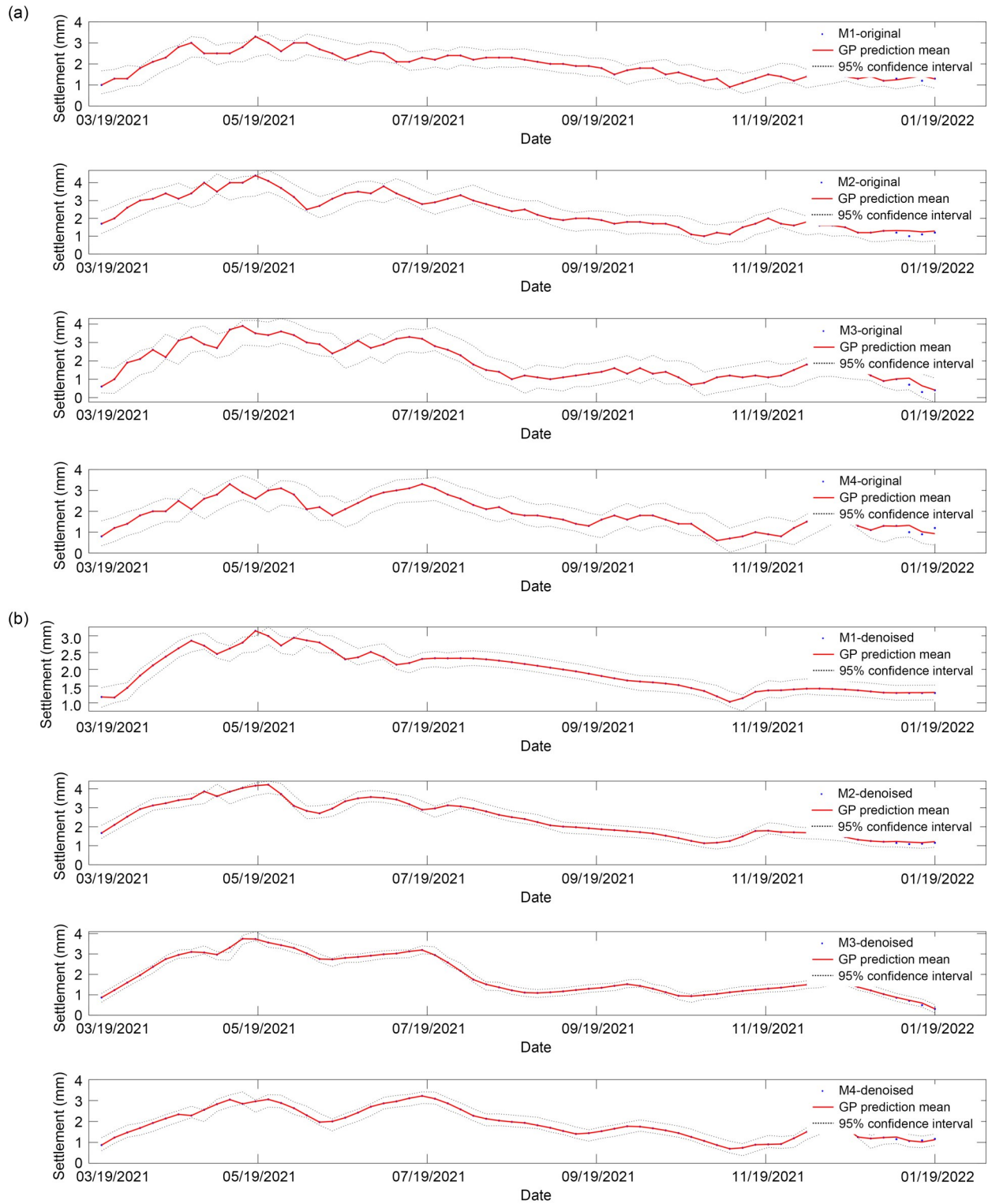


Fig. 7 Settlement probability prediction with a moving window of 5 and predicted ratio of 5%: (a) probability prediction based on original data; (b) probability prediction based on denoised data

model in quantitative settlement prediction (Ye et al., 2020).

$$RMSE = \sqrt{\frac{1}{N} \sum_{i=1}^N (y_i - M_i)^2}, \quad (7)$$

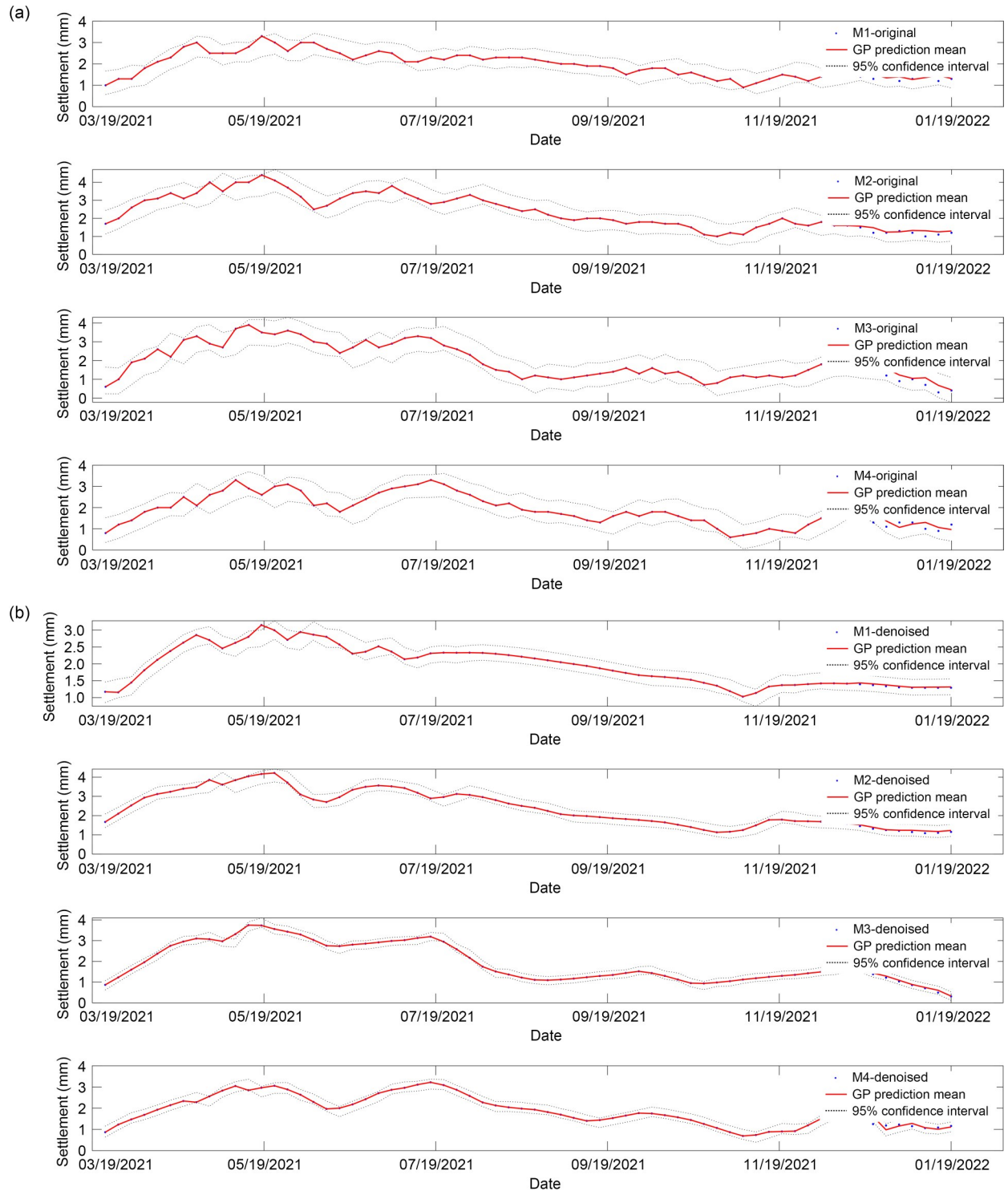


Fig. 8 Settlement probability prediction with a moving window of 5 and predicted ratio of 10%: (a) probability prediction based on original data; (b) probability prediction based on denoised data

where y_i is the predicted settlement, and M_i is the measured settlement.

Figs. 12–15 compare the prediction performances for the original data and denoised data using the GPBE

model, with different moving windows. The figures demonstrate that as the prediction proportion increases, the prediction performance of the proposed GPBE model gradually deteriorates. This is because higher

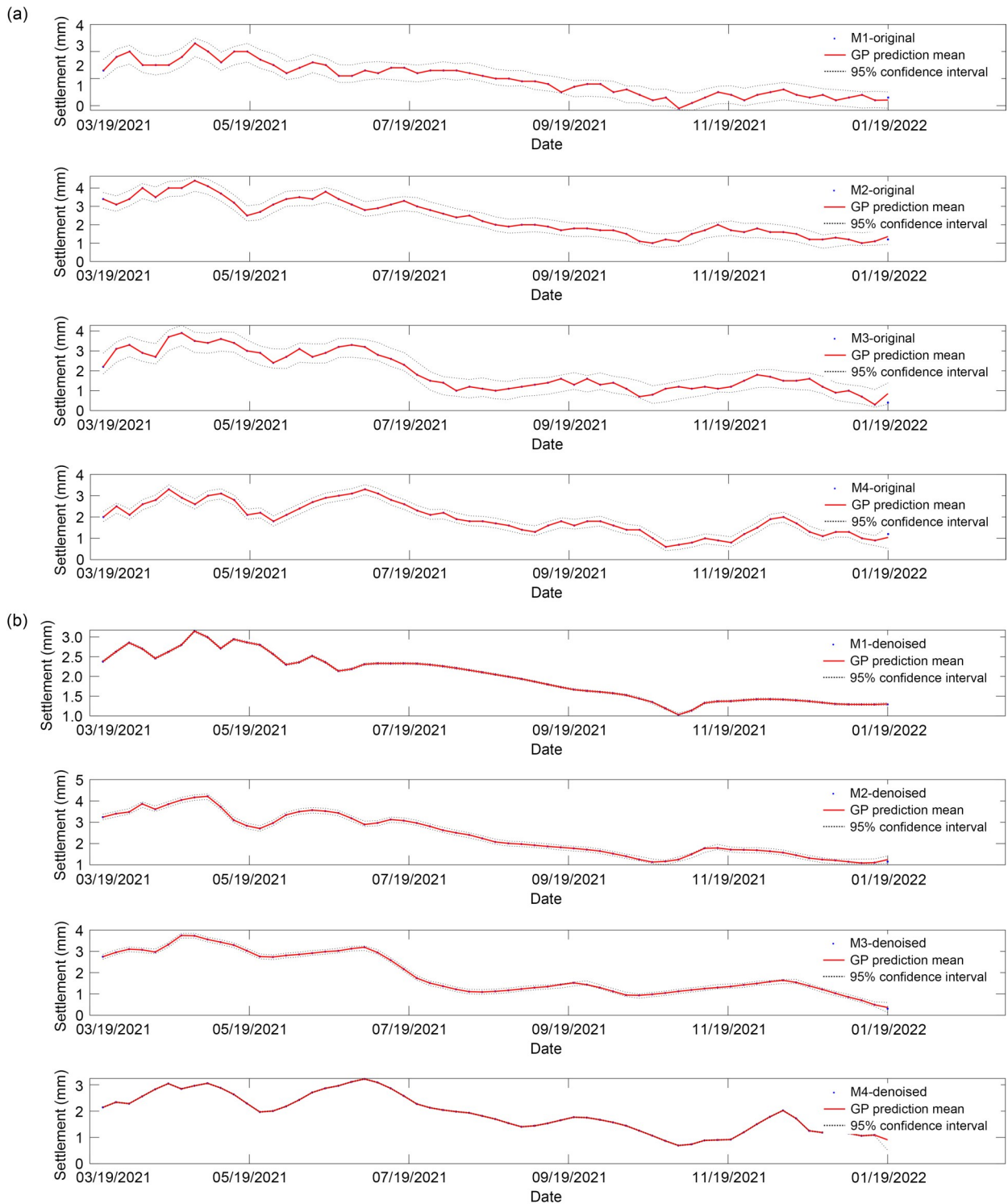


Fig. 9 Settlement probability prediction with a moving window of 10 and predicted ratio of 1%: (a) probability prediction based on original data; (b) probability prediction based on denoised data

prediction ratios lead to a decrease in the ratios of the training set, which prevent full mining of the information in the measured data. In addition, different moving

windows have different effects on prediction performance because the robustness of moving windows is unstable. The comprehensive calculation results show

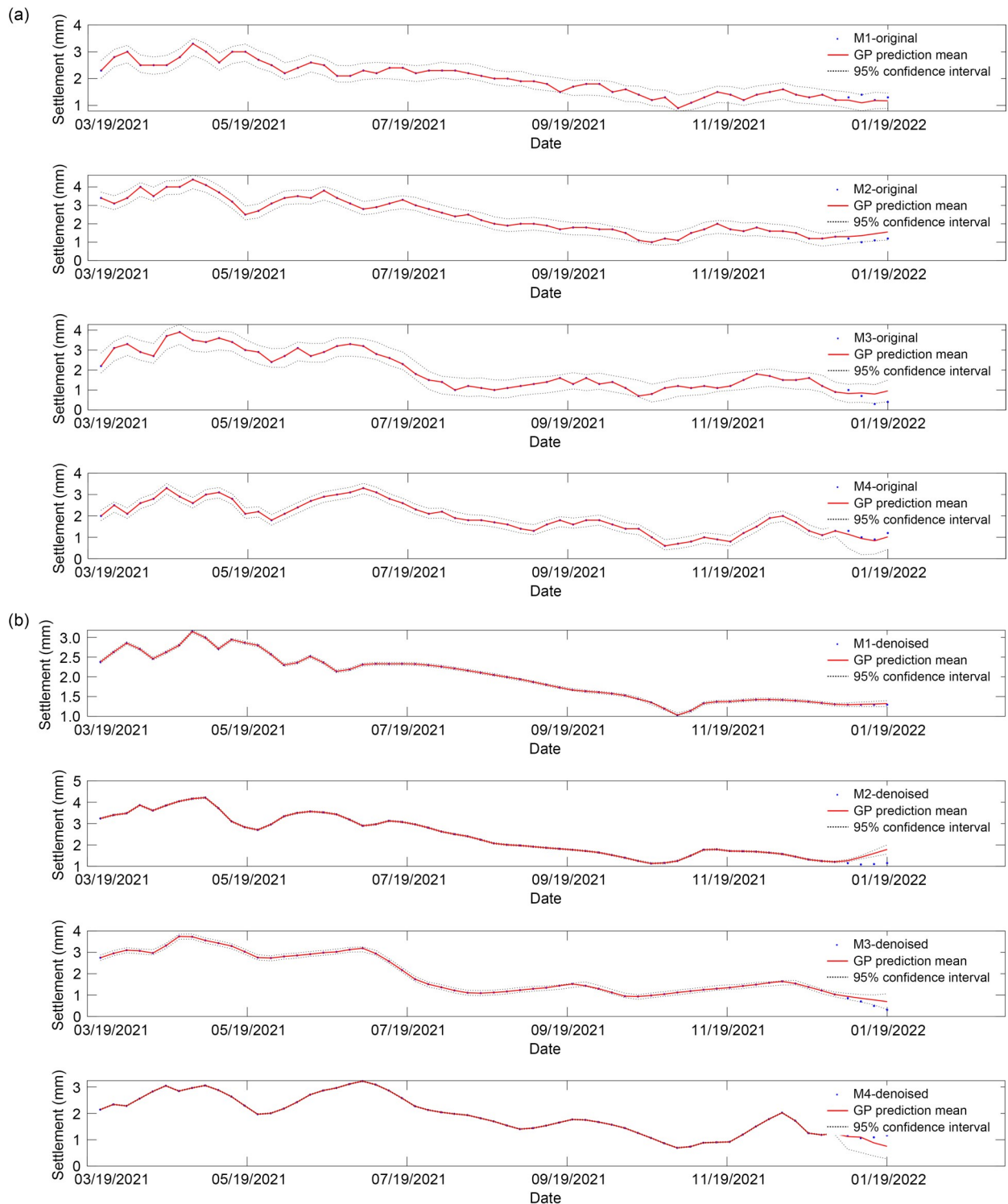


Fig. 10 Settlement probability prediction with a moving window of 10 and predicted ratio of 5%: (a) probability prediction based on original data; (b) probability prediction based on denoised data

that a moving window of 5 provides the best prediction performance in the proposed model. Meanwhile, the prediction performance of the proposed model is

worse for the original data than for the denoised data produced by WD; the settlement-prediction performance based on WD-GPBE is the best.

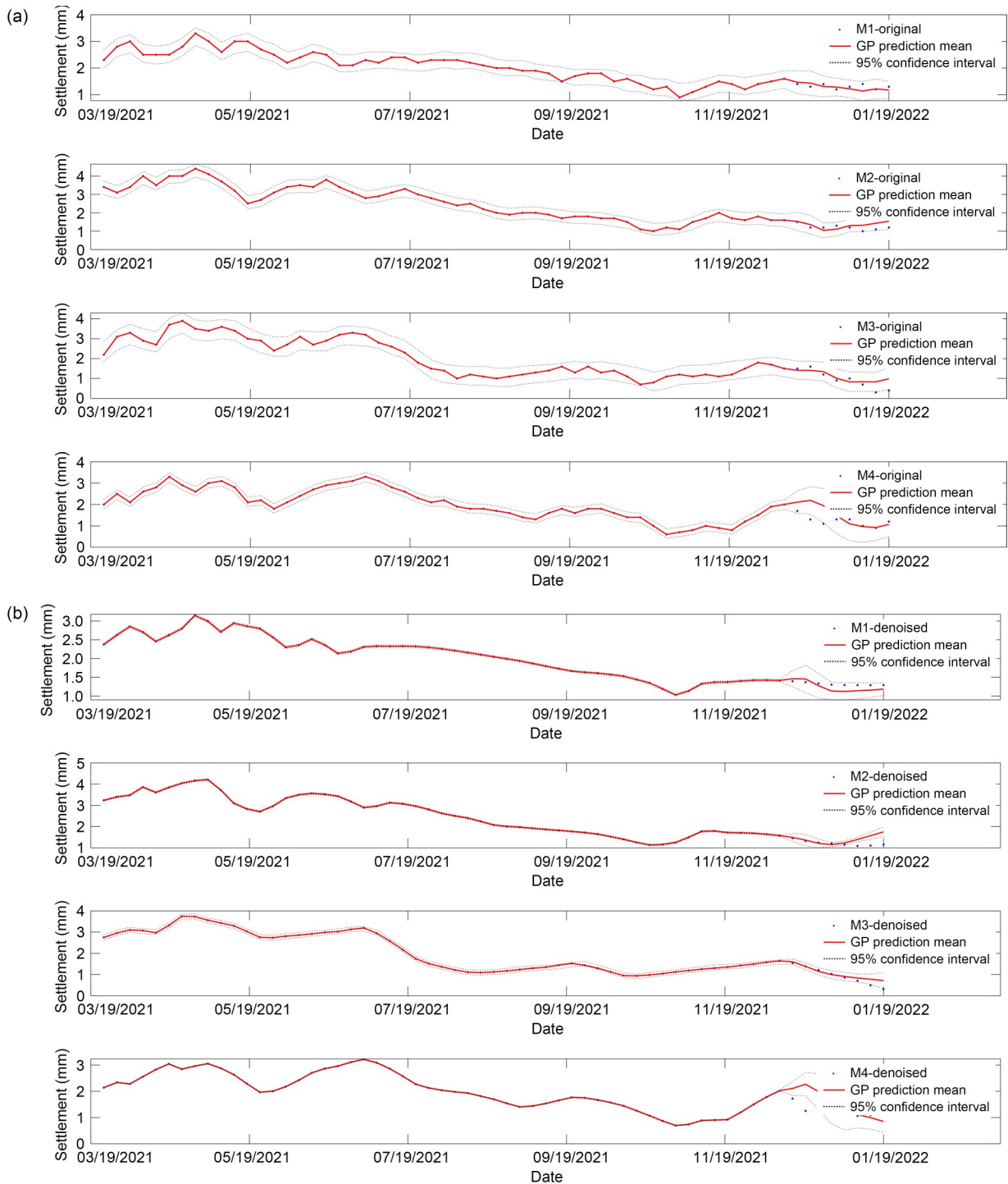


Fig. 11 Settlement probability prediction with a moving window of 10 and predicted ratio of 10%: (a) probability prediction based on original data; (b) probability prediction based on denoised data

4 Conclusions

In this paper, we propose a probability settlement-prediction model with a BE based on the GP with

WD, that is, WD-GPBE. A BE probability-prediction model based on GP is derived based on the Bayesian theorem. We discuss the effects of prediction proportion and moving windows on the model's prediction

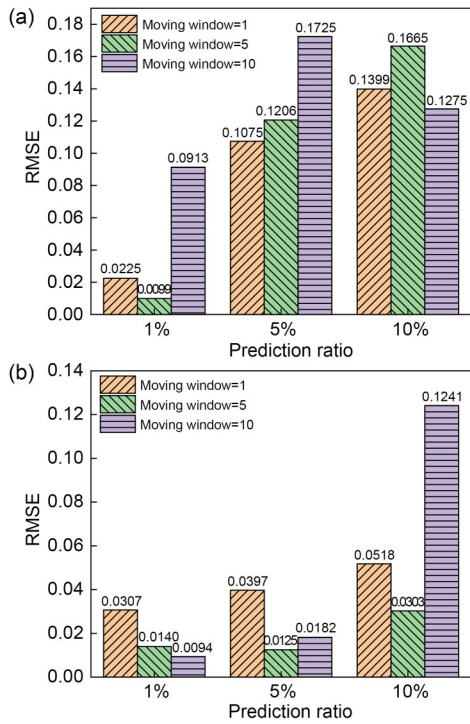


Fig. 12 Influence of moving window and prediction ratios on prediction performance with M1 data: (a) RMSE of M1-original data with GPBE; (b) RMSE of M1-denoised data with GPBE

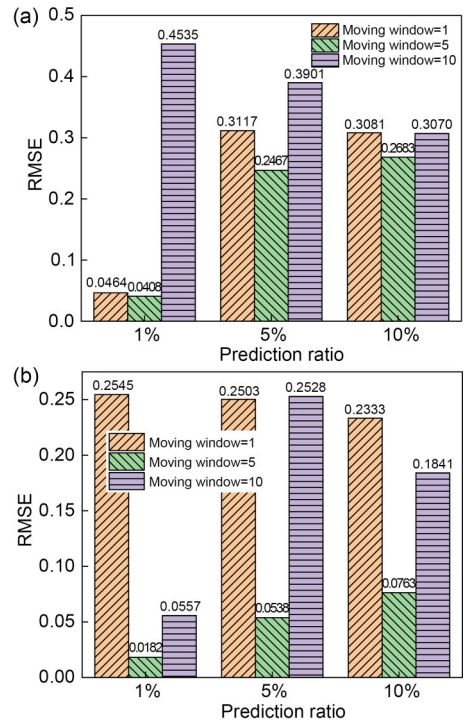


Fig. 14 Influence of moving window and prediction ratios on prediction performance with M3 data: (a) RMSE of M3-original data with GPBE; (b) RMSE of M3-denoised data with GPBE

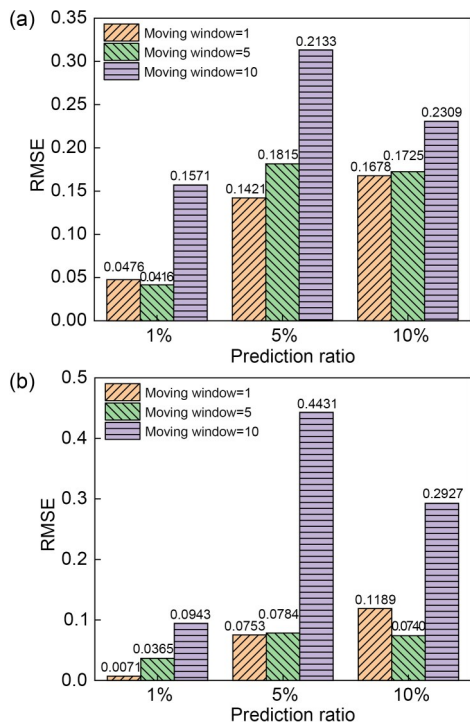


Fig. 13 Influence of moving window and prediction ratios on prediction performance with M2 data: (a) RMSE of M2-original data with GPBE; (b) RMSE of M2-denoised data with GPBE

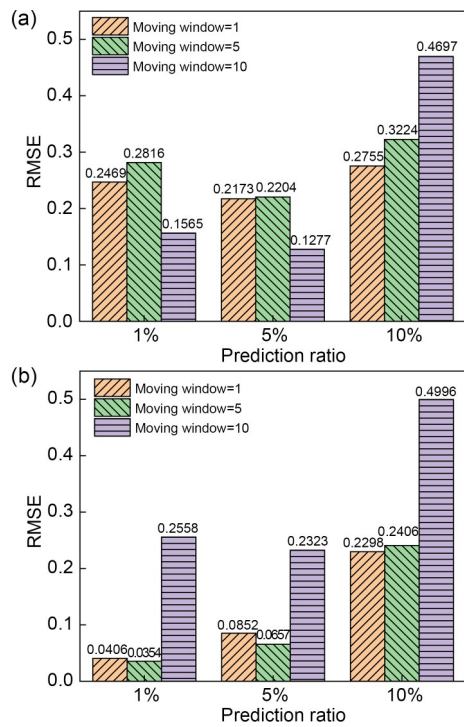


Fig. 15 Influence of moving window and prediction ratios on prediction performance with M4 data: (a) RMSE of M4-original data with GPBE; (b) RMSE of M4-denoised data with GPBE

performance. Furthermore, we compare the prediction performances of GPBE and WD-GPBE models, and verify them based on SHM data from the Nanjing Metro. Some conclusions are as follows:

(1) The proposed GPBE probability-prediction model can obtain the development law of settlement and predict settlement change well. The settlement change is within the 95% confidence interval, and thus fully describes the uncertainty of settlement.

(2) The larger the prediction ratios of settlement, the worse the prediction performance of the GPBE model. A moving window of 5 offers the best prediction performance within the model.

(3) The prediction performance of the WD-GPBE model is better than that of the GPBE model, demonstrating that it is necessary to denoise the original settlement-monitoring data before using it in the model.

In future research, we will analyze how to use the proposed model to evaluate the safety status (the useful life) of tunnel structures and improve the settlement warning function.

Acknowledgments

This work is supported by the Humanities and Social Sciences Research Project of Ministry of Education of China (No. 23YJ CZH037), the Educational Science Planning Project of Zhejiang Province (No. 2023SCG222), the Foundation of the State Key Laboratory of Mountain Bridge and Tunnel Engineering of China (No. SKLBT-2210), the National Key R&D Program of China (No. 2022YFC3802301), the National Natural Science Foundation of China (No. 52178306), and the Scientific Research Project of Zhejiang Provincial Department of Education (No. Y202248682), China.

Author contributions

Yang DING designed the research. Yang DING and Zhen HAN processed the corresponding data. Yang DING wrote the first draft of the manuscript. Zhi DING, Gang WEI, and Yunliang CUI helped to organize the manuscript. Yang DING, Xiaowei YE, and Tao JIN revised and edited the final version.

Conflict of interest

Yang DING, Xiaowei YE, Zhi DING, Gang WEI, Yunliang CUI, Zhen HAN, and Tao JIN declare that they have no conflict of interest.

References

- Chen RP, Zhang P, Wu HN, et al., 2019. Prediction of shield tunneling-induced ground settlement using machine learning techniques. *Frontiers of Structural and Civil Engineering*, 13(6):1363-1378.
- Cheng Y, Ye XF, Fujiyama T, 2020. Identifying crowding impact on departure time choice of commuters in urban rail transit. *Journal of Advanced Transportation*, 2020:8850565. <https://doi.org/10.1155/2020/8850565>
- Chitsazan N, Nadiri AA, Tsai FTC, 2015. Prediction and structural uncertainty analyses of artificial neural networks using hierarchical Bayesian model averaging. *Journal of Hydrology*, 528:52-62. <https://doi.org/10.1016/j.jhydrol.2015.06.007>
- Ding LY, Ma L, Luo HB, et al., 2011. Wavelet analysis for tunneling-induced ground settlement based on a stochastic model. *Tunnelling and Underground Space Technology*, 26(5):619-628. <https://doi.org/10.1016/j.tust.2011.03.005>
- Ding Y, Ye XW, Guo Y, 2023a. Data set from wind, temperature, humidity and cable acceleration monitoring of the Jiashao bridge. *Journal of Civil Structural Health Monitoring*, 13(2-3):579-589. <https://doi.org/10.1007/s13349-022-00662-5>
- Ding Y, Hang D, Wei YJ, et al., 2023b. Settlement prediction of existing metro induced by new metro construction with machine learning based on SHM data: a comparative study. *Journal of Civil Structural Health Monitoring*, in press. <https://doi.org/10.1007/s13349-023-00714-4>
- Ding Y, Ye XW, Guo Y, 2023c. A multistep direct and indirect strategy for predicting wind direction based on the EMD-LSTM model. *Structural Control and Health Monitoring*, 2023:4950487. <https://doi.org/10.1155/2023/4950487>
- Ding Y, Ye XW, Guo Y, et al., 2023d. Probabilistic method for wind speed prediction and statistics distribution inference based on SHM data-driven. *Probabilistic Engineering Mechanics*, 73:103475. <https://doi.org/10.1016/j.probenmech.2023.103475>
- Ding Y, Ye XW, Guo Y, 2023e. Copula-based JPDP of wind speed, wind direction, wind angle, and temperature with SHM data. *Probabilistic Engineering Mechanics*, 73:103483. <https://doi.org/10.1016/j.probenmech.2023.103483>
- Ding Y, Ye XW, Guo Y, 2023f. Wind load assessment with the JPDP of wind speed and direction based on SHM data. *Structures*, 47:2074-2080. <https://doi.org/10.1016/j.istruc.2022.12.028>
- Ding Y, Ye XW, Su YH, et al., 2023g. A framework of cable wire failure mode deduction based on Bayesian network. *Structures*, 57:104996. <https://doi.org/10.1016/j.istruc.2023.104996>
- Farrar CR, Park G, Allen DW, et al., 2006. Sensor network paradigms for structural health monitoring. *Structural Control and Health Monitoring*, 13(1):210-225. <https://doi.org/10.1002/stc.125>
- Gómez J, Casas JR, Villalba S, 2020. Structural health monitoring with distributed optical fiber sensors of tunnel lining affected by nearby construction activity. *Automation in Construction*, 117:103261. <https://doi.org/10.1016/j.autcon.2020.103261>
- Gong WP, Luo Z, Juang CH, et al., 2014. Optimization of site exploration program for improved prediction of tunneling-induced ground settlement in clays. *Computers and Geotechnics*, 56:69-79.

- <https://doi.org/10.1016/j.compgeo.2013.10.008>
Hashemi M, Beheshti S, 2010. Adaptive noise variance estimation in BayesShrink. *IEEE Signal Processing Letters*, 17(1):12-15.
<https://doi.org/10.1109/LSP.2009.2030856>
- Hashemi M, Beheshti S, 2014. Adaptive Bayesian denoising for general Gaussian distributed signals. *IEEE Transactions on Signal Processing*, 62(5):1147-1156.
<https://doi.org/10.1109/TSP.2013.2296272>
- He XH, Fang J, Scanlon A, et al., 2010. Wavelet-based non-stationary wind speed model in Dongting lake cable-stayed bridge. *Engineering*, 2(11):895-903.
<https://doi.org/10.4236/eng.2010.211113>
- Huang SX, Wang XP, Li CF, et al., 2019. Data decomposition method combining permutation entropy and spectral substitution with ensemble empirical mode decomposition. *Measurement*, 139:438-453.
<https://doi.org/10.1016/j.measurement.2019.01.026>
- Ji ZW, Wang B, Deng SP, et al., 2014. Predicting dynamic deformation of retaining structure by LSSVR-based time series method. *Neurocomputing*, 137:165-172.
<https://doi.org/10.1016/j.neucom.2013.03.073>
- Jiang XM, Mahadevan S, Adeli H, 2007. Bayesian wavelet packet denoising for structural system identification. *Structural Control and Health Monitoring*, 14(2):333-356.
<https://doi.org/10.1002/stc.161>
- Jiangsu Provincial Department of Housing and Urban Rural Development, 2015. Technical Specification for Monitoring Measurement of Urban Rail Transit Engineering in Jiangsu Province, DGJ32/J 195-2015. Jiangsu Provincial Department of Housing and Urban Rural Development, China (in Chinese).
- Kong LH, Wu ZC, Chen GH, et al., 2020. Crowdsensing-based cross-operator switch in rail transit systems. *IEEE Transactions on Communications*, 68(12):7938-7947.
<https://doi.org/10.1109/TCOMM.2020.3019527>
- Law YZ, Santo H, Lim KY, et al., 2020. Deterministic wave prediction for unidirectional sea-states in real-time using artificial neural network. *Ocean Engineering*, 195:106722.
<https://doi.org/10.1016/j.oceaneng.2019.106722>
- Li SH, Zhang MJ, Li PF, 2021. Analytical solutions to ground settlement induced by ground loss and construction loadings during curved shield tunneling. *Journal of Zhejiang University-SCIENCE A (Applied Physics & Engineering)*, 22(4):296-313.
<https://doi.org/10.1631/jzus.A2000120>
- Li X, Liu X, Li CZ, et al., 2019. Foundation pit displacement monitoring and prediction using least squares support vector machines based on multi-point measurement. *Structural Health Monitoring*, 18(3):715-724.
<https://doi.org/10.1177/1475921718767935>
- Liang JX, Tang XW, Wang TQ, et al., 2022. Numerical analysis of the influence of a river on tunnelling-induced ground deformation in soft soil. *Journal of Zhejiang University-SCIENCE A (Applied Physics & Engineering)*, 23(7):564-578.
<https://doi.org/10.1631/jzus.A2100683>
- Liu WF, Wu ZZ, Li CY, et al., 2022. Prediction of ground-borne vibration induced by a moving underground train based on excitation experiments. *Journal of Sound and Vibration*, 523:116728.
<https://doi.org/10.1016/j.jsv.2021.116728>
- MOHURD (Ministry of Housing and Urban-Rural Development of the People's Republic of China), 2013. Technical Code for Protection Structures of Urban Rail Transit, CJJ/T 202-2013. MOHURD, China (in Chinese).
- Mu BG, Xie XK, Li X, et al., 2021. Monitoring, modelling and prediction of segmental lining deformation and ground settlement of an EPB tunnel in different soils. *Tunnelling and Underground Space Technology*, 113:103870.
<https://doi.org/10.1016/j.tust.2021.103870>
- Ng CWW, Liu GB, Li Q, 2013. Investigation of the long-term tunnel settlement mechanisms of the first metro line in Shanghai. *Canadian Geotechnical Journal*, 50(6):674-684.
<https://doi.org/10.1139/cgj-2012-0298>
- Ni YQ, Wang YW, Zhang C, 2020. A Bayesian approach for condition assessment and damage alarm of bridge expansion joints using long-term structural health monitoring data. *Engineering Structures*, 212:110520.
<https://doi.org/10.1016/j.engstruct.2020.110520>
- Qu HF, Wang LH, Feng CL, et al., 2021. Study on deformation and stability of rock-like materials retaining structure during collaborative construction of super-adjacent underground project. *Advances in Materials Science and Engineering*, 2021:5558544.
<https://doi.org/10.1155/2021/5558544>
- Qu K, Xu YY, Huang JX, et al., 2023. Numerical simulation of hydrodynamic characteristics of submerged floating tunnels under the action of focused waves. *Journal of Changsha University of Science & Technology (Natural Science)*, (04):127-141 (in Chinese).
<https://doi.org/10.19951/j.cnki.1672-9331.20220425001>
- Samui P, 2008. Support vector machine applied to settlement of shallow foundations on cohesionless soils. *Computers and Geotechnics*, 35(3):419-427.
<https://doi.org/10.1016/j.compgeo.2007.06.014>
- Sandham W, Hamilton D, Fisher A, et al., 1998. Multiresolution wavelet decomposition of the seismocardiogram. *IEEE Transactions on Signal Processing*, 46(9):2541-2543.
<https://doi.org/10.1109/78.709542>
- Sendur L, Selesnick IW, 2002. Bivariate shrinkage functions for wavelet-based denoising exploiting interscale dependency. *IEEE Transactions on Signal Processing*, 50(11):2744-2756.
<https://doi.org/10.1109/TSP.2002.804091>
- Shahin MA, Jaksa MB, Maier HR, 2005. Neural network based stochastic design charts for settlement prediction. *Canadian Geotechnical Journal*, 42(1):110-120.
<https://doi.org/10.1139/T04-096>
- Sysyn M, Nabochenko O, Kovalchuk V, 2020a. Experimental investigation of the dynamic behavior of railway track with sleeper voids. *Railway Engineering Science*, 28(3):290-304.
<https://doi.org/10.1007/s40534-020-00217-8>
- Sysyn M, Gerber U, Kluge F, et al., 2020b. Turnout remaining useful life prognosis by means of on-board inertial measurements on operational trains. *International Journal of Rail Transportation*, 8(4):347-369.

- <https://doi.org/10.1080/23248378.2019.1685918>
- Sysyn M, Przybylowicz M, Nabochenko O, et al., 2021a. Identification of sleeper support conditions using mechanical model supported data-driven approach. *Sensors*, 21(11):3609. <https://doi.org/10.3390/s21113609>
- Sysyn M, Przybylowicz M, Nabochenko O, et al., 2021b. Mechanism of sleeper-ballast dynamic impact and residual settlements accumulation in zones with unsupported sleepers. *Sustainability*, 13(14):7740. <https://doi.org/10.3390/su13147740>
- Tay DB, 2021. Sensor network data denoising via recursive graph median filters. *Signal Processing*, 189:108302. <https://doi.org/10.1016/j.sigpro.2021.108302>
- Wang CH, Wang K, Tang DF, et al., 2022. Spatial random fields-based Bayesian method for calibrating geotechnical parameters with ground surface settlements induced by shield tunneling. *Acta Geotechnica*, 17:1503-1519. <https://doi.org/10.1007/s11440-021-01407-2>
- Wang F, Gou BC, Qin YW, 2013. Modeling tunneling-induced ground surface settlement development using a wavelet smooth relevance vector machine. *Computers and Geotechnics*, 54:125-132. <https://doi.org/10.1016/j.compgeo.2013.07.004>
- Wang MS, van der Schaar M, 2006. Operational rate-distortion modeling for wavelet video coders. *IEEE Transactions on Signal Processing*, 54(9):3505-3517. <https://doi.org/10.1109/TSP.2006.879273>
- Wu YQ, Wang K, Zhang LZ, et al., 2018. Sand-layer collapse treatment: an engineering example from Qingdao Metro subway tunnel. *Journal of Cleaner Production*, 197:19-24. <https://doi.org/10.1016/j.jclepro.2018.05.260>
- Xiang YY, Jiang ZP, He HJ, 2008. Assessment and control of metro-construction induced settlement of a pile-supported urban overpass. *Tunnelling and Underground Space Technology*, 23(3):300-307. <https://doi.org/10.1016/j.tust.2007.06.008>
- Yao YP, Qi SJ, Che LW, et al., 2018. Postconstruction settlement prediction of high embankment of silty clay at Chengde airport based on one-dimensional creep analytical method: case study. *International Journal of Geomechanics*, 18(7):05018004. [https://doi.org/10.1061/\(ASCE\)GM.1943-5622.0001191](https://doi.org/10.1061/(ASCE)GM.1943-5622.0001191)
- Ye XW, Ding Y, Wan HP, 2019. Machine learning approaches for wind speed forecasting using long-term monitoring data: a comparative study. *Smart Structures and Systems*, 24(6):733-744. <https://doi.org/10.12989/sss.2019.24.6.733>
- Ye XW, Ding Y, Wan HP, 2020. Statistical evaluation of wind properties based on long-term monitoring data. *Journal of Civil Structural Health Monitoring*, 10(5):987-1000. <https://doi.org/10.1007/s13349-020-00430-3>
- Ye XW, Ding Y, Wan HP, 2021. Probabilistic forecast of wind speed based on Bayesian emulator using monitoring data. *Structural Control and Health Monitoring*, 28(1):e2650. <https://doi.org/10.1002/stc.2650>
- Zhang LM, Wu XG, Ji WY, et al., 2017. Intelligent approach to estimation of tunnel-induced ground settlement using wavelet packet and support vector machines. *Journal of Computing in Civil Engineering*, 31(2):04016053. [https://doi.org/10.1061/\(ASCE\)CP.1943-5487.0000621](https://doi.org/10.1061/(ASCE)CP.1943-5487.0000621)